Kinetic Insights into Cadmium and Lead Removal Using Cellulose-Based Schiff Base Complexes as Adsorbents

Farah Muaiad Ibrahim*

Department of Chemistry, College of Science, Al-Nahrain University, Jadria, Baghdad 10072, Iraq

* ***Corresponding author:***

email: tahafarah77777@gmail.com

Received: February 25, 2025
Accepted: April 8, 2025

DOI: 10.22146/ijc.104991

Abstract: *The removal of heavy metals from water is a key environmental challenge. This study focuses on synthesizing and using Schiff base-modified cellulose as adsorbents for cadmium (Cd) and lead (Pb) ions. The materials were developed by modifying cellulose and incorporating Schiff base ligands with Fe(III) and Zn(II) binding sites (Schiffs 1 and 2). Characterization through EDX, SEM, FTIR, elemental analysis, XRD, and TGA confirmed improved surface properties and active adsorption sites. Adsorption followed pseudo-second-order kinetics, indicating chemisorption. The monolayer adsorption capacities for Schiff 1 were 83 mg/g Cd and 78 mg/g Pb, while for Schiff 2, they were 70 mg/g Cd and 63 mg/g Pb. Optimal conditions included solution pH 4.0–5.0, stirring for 45–60 min, 100 mg/L metal concentration, and room temperature (25 ± 2 °C). EDTA efficiently desorbed Cd and Pb for 4 cycles with over 85% efficiency. This study highlights the material's potential as a cost-effective and eco-friendly solution for wastewater treatment.*

Keywords: *Schiff base; ion exchange; cadmium ion; lead ion; environmental remediation*

■ INTRODUCTION

The ongoing pollution of water bodies with heavy metals is a serious threat to environmental and human health integrity, largely due to their toxic, persistent, and bio-accumulative nature. Heavy metal influx into aquatic systems is largely attributed to industrial activities like mining, electroplating, and manufacturing [1-2]. Perhaps the most poisonous metal, lead (Pb), enters water bodies through industrial effluent, rusty pipes, and mining. Chronic exposure to Pb has been linked with neurological disease, dwarfism in children, renal failure, and circulatory dysfunction in adults [3]. Commonly released into the environment by industrial effluent, agricultural runoff, and electroplating, cadmium (Cd) poses a serious risk to human health due to its carcinogenicity and kidney damage. Poor bone formation, and oncogenicity are among the major health risks associated with Cd, which is inevitably released into the environment through industrial effluents, agricultural runoff, and electroplating operations [4-6]. Conventional remediation processes, like chemical precipitation and solvent extraction, are inefficient as well as economically unfavorable for trace metal concentration removal in most cases [7]. Consequently, studies are now focused on the search for efficient and sustainable sorbents for the removal of heavy metals from aqueous solution. Adsorption has been projected as an alternative process that is easy, highly efficient, and reusable. Using modified natural materials as sorbents was found to be a successful and sustainable approach [8-10].

Cellulose, being the most widely occurring natural polymer, has also proven to be a good sorbent due to the fact that it is renewable, biodegradable, and structurally flexible [11]. Unmodified cellulose does not possess sufficient active sites for efficient metal ion adsorption, but it is accomplished with chemical modifications and the incorporation of functional groups to bring about enhancement in adsorption efficiency. One such pivotal approach is inclusion of Schiff base parts, which have been observed to exhibit striking metal ion chelating ability. Schiff base complexes formed through condensation of primary amines with carbonyl compounds feature imine functional groups (C=N) having very high metal ion affinities [12]. All the alterations make cellulose a good and selective adsorbent for adsorption of heavy metals. Cellulose functionalized

with carboxylic acid and Schiff base groups is likely to improve metal adsorption because of the higher number of binding sites. Current research is focused on optimizing the potential of cellulose-based sorbents by incorporating valuable Schiff base derivatives and hybrid materials [13]. A prime example is the synthesis of chitosan-di-aldehyde cellulose hybrids via Schiff base reactions, which has resulted in sorbents with improved mechanical stability and higher heavy metal adsorption capacity. Such advances highlight the enormous potential of chemically modified naturally occurring polymers in solving environmental pollution issues [14-15]. Moreover, kinetic studies are valuable in understanding the efficacy and mechanisms of adsorption processes. Using kinetic adsorption examination and extrapolating experimental results to kinetic models, investigators can provide information concerning the tendencies in adsorbate-sorbent interaction [16].

While cellulose-Schiff base (CSB) modified cellulose materials exhibited pseudo-second-order kinetic behavior, which is often associated with chemisorption [17], additional investigations are necessary to fully elucidate the adsorption mechanism. Diffusion coefficients and activation energy are related to transport kinetics and energy barriers for adsorption. Kinetic study under strict conditions of such modified materials remains a less studied research area in the realm of investigation.

Here, the synthesis of new CSB sorbents with iron (Schiff 1) and zinc (Schiff 2) is presented. Removal of Cd and Pb ions from simulated wastewater and wastewater by the sorbents was evaluated. SEM, EDX, TGA, FTIR, and elemental analysis were applied to analyze both sorbents. Using the batch process, the role of pH, time, initial concentration of ions, and temperature adsorption was analyzed. Adsorption kinetics and desorption in regeneration experiments were examined.

■ EXPERIMENTAL SECTION

Materials

Cellulose ($(C_6H_{10}O_5)_n$, 99%), phosphorous oxychloride ($POCl_3$, 99%), ethanol (C_2H_6O, 99.8%), dimethylformamide (DMF, 99.8%), tetraethylenepentamine (TEPA, 95%), thiourea (CH_4N_2S, 99%), ethylene diamine tetracetic acid (EDTA, 99%), iron chloride ($FeCl_3$, 98%), zinc chloride ($ZnCl_2$, 98%), NaOH (98%), and HNO_3 (70%) were Aldrich products. All additional material was utilized exactly as received; all chemicals were Prolabo products. Metal ion sources included Cd and Pb solutions with a concentration of 1000 ppm.

Instrumentation

The functional groups of the synthesized sorbent were identified using a Bomen Michelson Fourier transform infrared (FTIR) spectrophotometer, model MB157 (Canada). The crystalline structure was analyzed with a Shimadzu X-ray diffraction (XRD) instrument, model XD-DL (Kyoto, Japan), covering a diffraction angle (2θ) range of 4–70°. Thermal analysis was performed to assess phase transitions and mass variations within a temperature range from ambient conditions up to 650 °C. The surface morphology of the prepared sorbent was characterized using a JEOL JSM-5400 scanning electron microscope (SEM, Japan) and a FEI Quanta FEG-250 system equipped with energy-dispersive X-ray spectroscopy (EDX). Elemental analysis was carried out using Perkin Elmer 2400 CHN elemental analyzer. ICP (720 ICP-OES, Agilent Technologies) was used to assess the metal ions under study. Using an Adwic pH meter, the concentration of hydrogen ions in the various solutions was determined.

Procedure

Synthesis of the CSB and its metal complexes

Preparation of CSB. First, 10 g of cellulose were combined with 200 mL of DMF and allowed to stand for 1 h. Subsequently, 18 mL of $POCl_3$ were introduced into the mixture and subjected to mechanical stirring for over 15 min. The resulting cellulose chloride (Cell-Cl) was isolated via filtration and thoroughly washed with DMF, distilled water, and a 5% NaOH solution. It was then rinsed again with distilled water and air-dried. In a separate step, 42 mL of TEPA and 14 g of thiourea were refluxed in a DMF medium at 60 °C for 3 h. Following this, 10 g of Cell-Cl were added to the mixture under continuous stirring. The reaction mixture was heated to

80 °C and stirred for 5 h. The final product, modified CSB, was obtained after filtration, washing with distilled water and ethanol, and air-drying. Fig. 1 represents a simplified flowchart for CSB preparation. The CSB preparation could be expressed according to Eq. (1–3) [18].

$$\text{Cellulose–OH} + POCl_3 \rightarrow \text{Cell–Cl} + HPOCl_2 \quad (1)$$

$$\text{TEPA} + \text{Thiourea (heat)} \rightarrow \text{Intermediate product(s)} \quad (2)$$

$$\text{Intermediate product(s)} + \text{Cell–Cl (heat)} \rightarrow \text{CSB} \quad (3)$$

Synthesis of metal complexes. To synthesize Schiff base adsorbent 1, 5.0 g of CSB were dissolved in 50 mL of absolute ethanol. This solution was then added dropwise, under constant stirring, to 30 mL of an ethanolic solution containing 2.5 g of anhydrous $ZnCl_2$. The reaction mixture was stirred in a closed system at 50 °C for 4 h to ensure complete reaction. The resulting precipitate (Schiff 1) was then filtered, washed with distilled water, and dried at room temperature.

For Schiff base adsorbent 2, the same procedure was followed, with the exception that 2.5 g of anhydrous $FeCl_3$ were used instead of $ZnCl_2$. Specifically, 5.0 g of CSB were dissolved in 50 mL of absolute ethanol. This solution was added dropwise to 30 mL of an ethanolic solution containing 2.5 g of $FeCl_3$, under constant stirring. The reaction mixture was stirred at 50 °C for 4 h. The resulting precipitate (Schiff 2) was then filtered, washed with distilled water, and dried at room temperature.

Chemical stability studies of prepared CSB

The chemical stability of the synthesized adsorbent in both acidic and alkaline environments was evaluated by independently immersing a measured quantity of CSB in 100 mL of varying concentrations of NaOH and HNO_3 (0.5 and 1 mol/L). The CSB was soaked for 24 h in each medium, after which its stability was determined. The prepared Schiff base was filtered, dried, and assessed for structural integrity and performance.

Adsorption batch experiments

A variety of experimental factors influencing the adsorption procedure were evaluated. Some of these factors were the initial concentrations of both heavy metal ions, the pH of the solution, and the duration of contact. Using HNO_3 or NaOH solutions (0.1 mol/L), the pH of the mixture was changed from 1.0 to 6.0. The adsorption investigations were completed in batches utilizing a hotplate magnetic stirrer and 25 mg sample sections of Schiffs 1 and 2, separately combined with a specific volume of Cd or Pb ion solution in a 50 mL glass flask. Subsequently, the mixture was shaken at ambient temperature for 2 h. The remaining metal ion concentration was measured using ICP after equilibration. Schiffs 1 and 2 were separated by filtration. Eq. (4) was employed to estimate the adsorption capacity (q).

$$q = (C_{initial} - C_{final}) \times V/m \quad (4)$$

After each experiment was conducted three times, the standard deviation was employed to ascertain the averaged findings. The Cd and Pb solutions (25 mL solutions of 100 mg/L at pH 4.0 for Schiff 1 and 5.0 for Schiff 2) were treated with 25 mg of Schiff 1 and 2, separately at 25 °C with different shaking times from 15 up to 90 min. The effect of both elements ions was studied using various concentrations of 25–200 mg/L. The coexisting ions effect (Na, Ca, Ti, Cr, and V) with similar concentration with the target elements was evaluated. The efficacy of metal ion adsorption was assessed under the previously adjusted adsorption conditions.

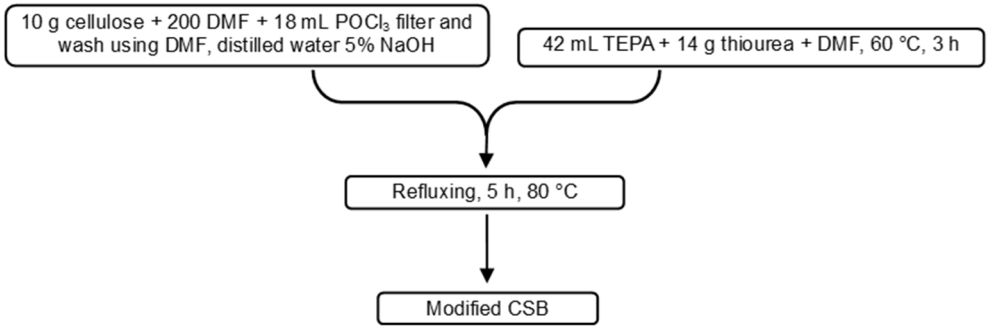

Fig 1. Flow chart for preparation of CSB

Adsorption kinetics

The adsorption kinetics were comprehensively examined in this section by using 25 mg of each adsorbent with 25 mL of pH 4.0 for Schiff 1 and pH 5.0 for Schiff 2, with feed solutions containing the ions of the studied elements at concentrations from 25 to 200 mg/L of each component independently. The feed solution and adsorbents were agitated in Cd and Pb solutions for 45 and 60 min. Four distinct stirring temperatures between 25 and 50 °C were used for the experiments, which were carried out in a glass flask. Plotting the adsorption isotherms for Pb and Cd on Schiff 1 and 2 was done using the adsorption efficiency percentage, which was determined using Eq. (5) and (6) following each test. The adsorption kinetics of Schiff 1 and 2 adsorbents for Cd(II) and Pb(II) ions were calculated by analyzing the stirring time parameters. Two kinetic models, pseudo-first-order and pseudo-second-order, were used [19].

$$\log(q_e - q_t) = \log q_e - \left(\frac{k_1}{2.303}\right)t \quad (5)$$

$$\frac{t}{q_t} = \frac{1}{k_2 q_e^2} + \frac{1}{q_e}t \quad (6)$$

Desorption and regeneration studies

By separately contacting the loaded adsorbents with various eluents at a concentration of 0.5 mol/L, such as H_2SO_4, HCl, and HNO_3, as well as EDTA, Cd(II) and Pb(II) desorption from the loaded Schiff 1 and 2 adsorbents was carried out. The desorption conditions were standardized to a 30-min stirring duration, 20 mL of eluent solution, 40 mg of loaded adsorbents, and a stirring rate of 250 rpm at ambient temperature. Both adsorbents were filtered post-experiment and the remaining eluents were analyzed thoroughly for Cd and Pb ion content to determine optimal desorption conditions. The two adsorbents' regeneration efficiencies (%) were calculated using a defined equation Eq. (7) by repeating the adsorption/desorption cycles;

$$\text{Regeneration efficiency (\%)} = \frac{\text{Target elements recovery in } (n+1)^{th} \text{ run}}{\text{Target element recovery in } 1^{st} \text{run}} \times 100\% \quad (7)$$

where n = 1, 2, or 3, etc. After each cycle, the sorbents were rinsed with distilled water and reused for subsequent adsorption operations. The optimal adsorption and desorption parameters were applied in the adsorption/desorption process.

Evaluation using actual raffinate solutions

Testing Schiff 1 and 2 on waste solution. Raffinate solution was collected from Glass and Ceramics Company, as Pb is used in glass manufacturing, including leaded glass and crystal products. In contrast, Cd is used in glass coloring agents and ceramic glazes. Substantial concentrations of Cd(II) and Pb(II) were identified in this real solution. The retrieval of these target elements was examined using the synthesized adsorbents, following the previously established adsorption parameters.

■ RESULTS AND DISCUSSION

Evaluation of the Schiffs 1 and 2 Adsorbents

XRD results

The XRD patterns of the two adsorbents are presented in Fig. 2 with the Schiff 1 curve representing the CSB modified with Fe and the Schiff 2 curve corresponding to the CSB attached to Zn(II) ions. Schiff 1 pattern exhibits characteristic peaks at approximately 35.4 and 43.1°, corresponding to the (311) and (400) planes of Fe, confirming the successful incorporation of Fe particles [20-22]. In contrast, the Schiff 2 pattern showed a notable peak near 22.6°, which may be associated with Zn(II) ions coordinated to the Schiff base

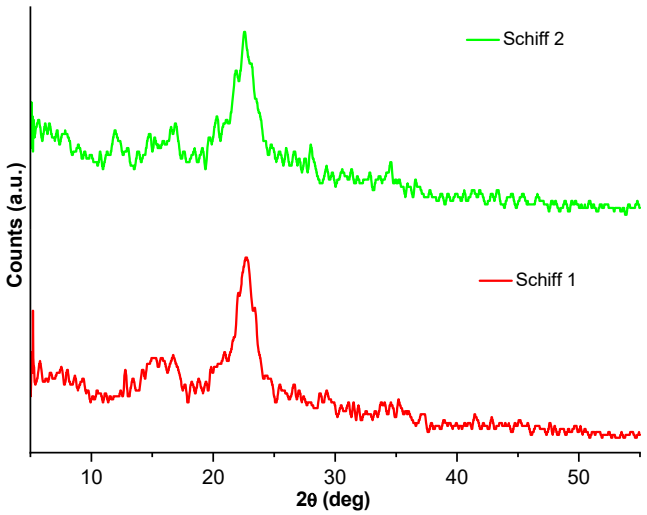

Fig 2. XRD pattern of the Schiffs 1 and 2 adsorbents

structure or the formation of a Zn-containing phase [23]. The broad background signals in both patterns reflected the semi-crystalline nature of the cellulose matrix, while the sharp peaks confirmed the respective modifications with Fe and Zn(II) ions. There is noticeable similarity in XRD patterns which suggested that the overall crystalline structure of the CSB was largely maintained after the metal complexation. The absence of distinct Fe peaks in Schiff 1 could be related to that the Fe is likely dispersed amorphously or in very small crystalline domains, which are below the detection limit of XRD analysis.

EDX results

The EDX analysis of the two prepared adsorbents (Fig. 3) revealed several key elemental features. The prominent peaks corresponding to carbon (C) and oxygen (O) were indicative of the cellulose backbone, indicating the presence of hydroxyl groups and the polysaccharide structure, as expected for organic polymeric materials [24-25]. The presence of nitrogen (N) and sulfur (S) in the spectrum confirmed the incorporation of the amine and thiourea groups as imine (C=N) linkages [26], which play a crucial role in the formation of the Schiff base structure [27-28]. For Schiff 1, The Fe-specific peak at 6.4 keV (Fe K_α) further verifies the successful coordination of Fe ions within the Schiff base structure, suggesting that Fe is integrated into the adsorbent [29]. Otherwise, for Schiff 2, the distinct peak for Zn around 8.6 keV (Zn K_α) confirmed the attachment of Zn(II) ions to the CSB matrix. The intensity of the Zn signal reflects effective coordination between the Schiff base ligands and Zn(II) ions facilitated by the electron-donating imine nitrogen atoms. This functionalized material demonstrates potential for applications in adsorption, catalysis, or as an antimicrobial agent due to the known activity of Zn-based compounds. A peak for phosphorus (P), which is at about 2.01 keV, indicates residual phosphate groups or phosphorus-containing reactants from the synthesis procedure. Indicated Cl peak may be attributed to chemicals or by-products in the functionalization process. The results indicate that the CSB adsorbent is a matrix with metal coupled with an organic polymeric composite, which most likely increases its efficiency in adsorbing a wide range of pollutants, including heavy metals [30-31].

FTIR data

Fig. 4 shows the FTIR spectrum of Schiff 1 and 2 adsorbents. The stretching vibrations of the hydroxyl (O–H) groups from the cellulose backbone are linked to a broad band seen in the 3200–3500 cm^{-1} range [32-33]. Imine bond formation (C=N), a characteristic of Schiff base ligands, is confirmed by a noticeable absorption peak

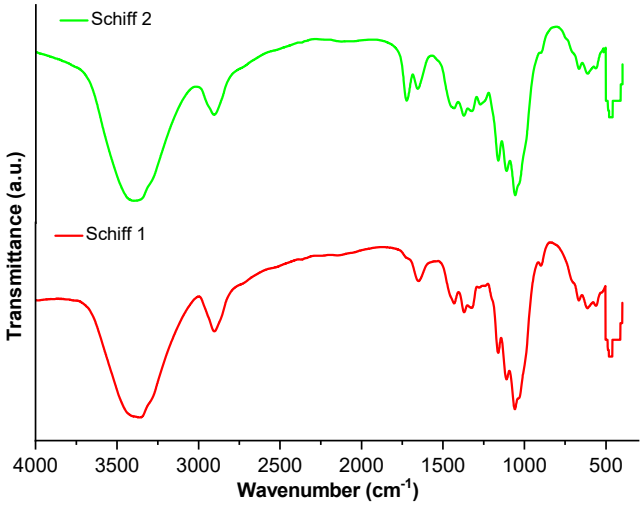

Fig 4. FTIR-spectra of Schiffs 1 and 2

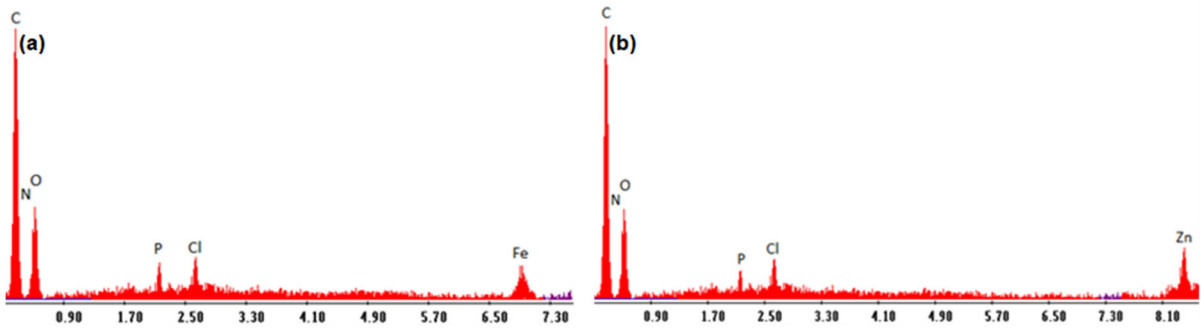

Fig 3. EDX-chart of the (a) Schiff 1 and (b) Schiff 2

in the 1600–1640 cm^{-1} region [8,34]. Its successful integration into the Schiff base framework is confirmed by additional peaks in the 1200–1400 cm^{-1} range that correspond to thiocarbamide (C=S or C–NH) groups produced from thiourea.

Metal coordination is directly demonstrated by distinct peaks in the 400–600 cm^{-1} area. Fe–N and Fe–S stretching vibrations are represented by bands in the range of 450–500 cm^{-1} for Fe-functionalized CSB. While, for Zn-functionalized materials, bands appeared at 430–500 cm^{-1} correlate to Zn–N and Zn–S stretching vibrations [35]. The cellulose backbone's peaks, including the (C–H) stretching (2800–3000 cm^{-1}) and the (C–O–C) vibrations (1100–1150 cm^{-1}) [36], are still there but could show slight changes as a result of the chemical changes.

TGA data

The TGA profiles of Schiffs 1 and 2 (Fig. 5) demonstrated distinct thermal decomposition patterns, significantly influenced by the specific metal ions (Fe or Zn) coordinated with the CSB. The initial weight loss observed below 150 °C for both adsorbents is attributed to the evaporation of physically adsorbed water and possibly residual solvent molecules from the synthesis process [37]. The primary decomposition phase for Schiff 1 occurred between approximately 200 and 400 °C, corresponding to the degradation of the CSB backbone and the cleavage of coordinated bonds with Fe ions. Similarly, Schiff 2 exhibited its significant weight loss in a comparable temperature range, albeit with slightly higher thermal stability than Schiff 1. The enhanced thermal stability in Schiff 2 may be attributed to the stronger bonding interactions between the zinc ions and the CSB, consistent with prior findings that zinc coordination complexes tend to exhibit higher thermal resistance than their Fe counterparts [38]. The final weight residues observed above 500 °C likely represented thermally stable metal oxides (Fe_2O_3 for Schiff 1 and ZnO for Schiff 2), which align with the thermal decomposition products commonly reported for metal-coordinated cellulose derivatives [39]. Overall, the results suggest that the nature of the metal ion plays a critical role in the thermal behavior of CSB complexes.

Adsorbent Morphology

The SEM images of the synthesized Schiff adsorbents are presented in Fig. 6(a) and 6(b). The SEM analysis indicated a textured surface morphology with heterogeneous particle distribution. The adsorbent

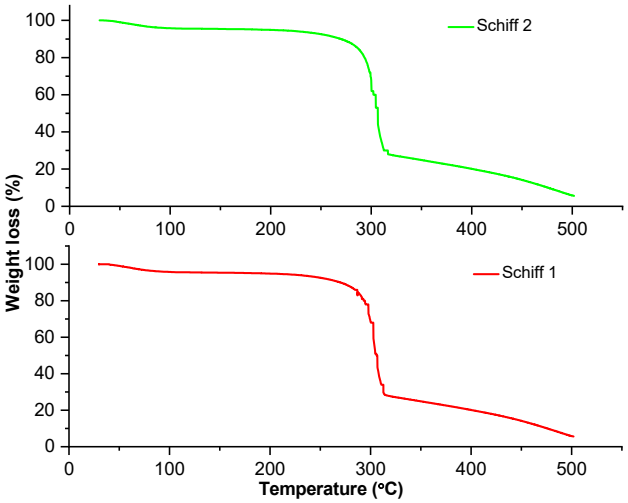

Fig 5. TGA chart of Schiffs 1 and 2

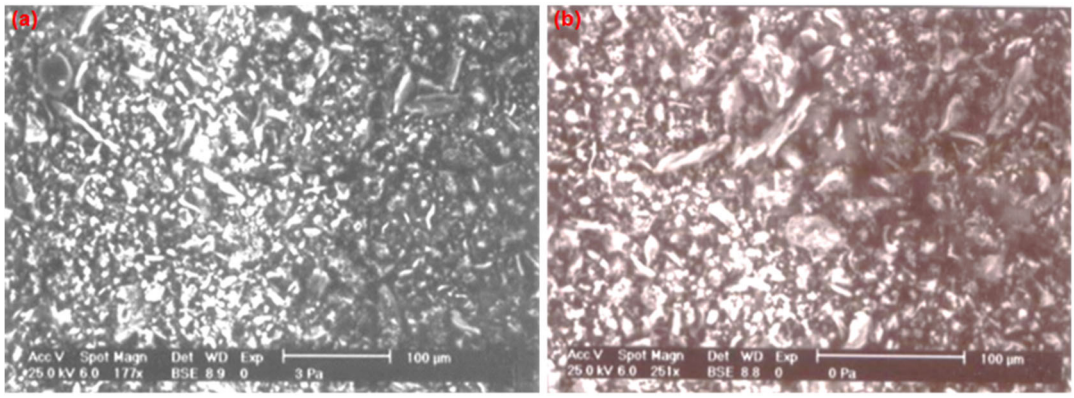

Fig 6. SEM images for (a) Schiff 1 and (b) Schiff 2 adsorbents

exhibited a structure composed of spherical particles of uniform size. The existence of multiple prominences and gaps between granules enhanced the adsorption effectiveness and promoted faster diffusion of the solution.

Elemental Analysis Data

The elemental analysis of CSB derived from the reaction between pentamine and thiourea in the presence of Fe and Zn ions separately provides insights into the composition and ion incorporation within the material. For Schiff 1, the N content (7.0%) corresponded to the amine and thiourea groups in the Schiff base, while the S content (1.8%) confirmed the presence of the thiourea functionality, while for Schiff 2 (7.3% and 1.5%, respectively). The proportions of C and H remained in alignment with the cellulose backbone, at 46.0% and 8.0% for Schiff 1, and 47.0% and 7.5% for Schiff 2. The elemental analysis in both cases confirmed the successful integration of metal ions into the cellulose, highlighting the dual functionality of these Schiff base adsorbents in eliminating heavy metals from water.

Data of Chemical Stability Analysis

The acid and alkaline stability of CSB was studied because of its importance in catalysis and adsorption applications. The modified CSB was discovered to be acid-stable due to the strong covalent bonding achieved upon modification. In alkaline media, however, the compound is destabilized via the possible degradation of the imine (C=N) bond, which is most degradable at high pH [40-41]. However, this problem can be addressed by incorporating functional groups and cross-linking agents in the process of modification to improve the stability and resistance of the material to alkaline conditions. The pH conditions have far-reaching effects on the stability of modified CSB, with acidic conditions poised to improve structural stability, but with alkaline conditions possibly needing additional modifications to advance durability. The pH-dependent character indicates the necessity of tailoring the material to applications in order to realize maximum efficiency.

Optimization of Adsorption Conditions

Influence of pH

A series of experiments were carried out to examine the effect of pH on the adsorption performance of Cd(II) and Pb(II) ions onto the two adsorbents. The pH levels in these experiments were changed from 1.0 to 6.0, while the experimental conditions were kept constant. The involved mechanism can be described using in the Eq. (8) [42];

$$CSB–M_1 + M_2 \rightarrow CSB–M_2 + M_1 \quad (8)$$

where M_1: Fe(III) or Zn(II) and M_2: Cd(II) or Pb(II)

The effect of pH on the ion exchange mechanism of CSB adsorbents attached to Fe and zinc is significant, as it influenced the protonation state of the adsorbent, the solubility of the metal ions, and the overall efficiency of the ion exchange process. As illustrated in Fig. 7(a) for Schiff 1, raising the pH of the aqueous phase from 1.0 to 6.0 led to a notable enhancement in the adsorption of both Cd(II) and Pb(II) ions onto the investigated adsorbent. The adsorbed quantities of Cd(II) and Pb(II)

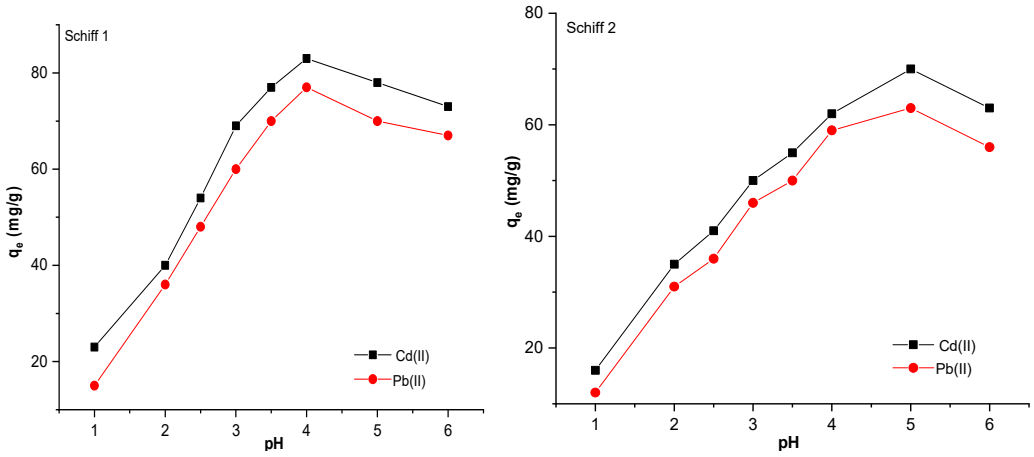

Fig 7. Effect of pH on the adsorption of Cd(II) and Pb(II) on Schiffs 1 and 2

ions increased from 23 and 15 to 83 and 77 mg/g, respectively. As a result, the optimal pH was typically 4.0. As a lower pH (< 4), CSB may become protonated, reducing its ability to coordinate with incoming metal ions, while at higher pH (> 6), Fe(III) tends to hydrolyze, forming insoluble $Fe(OH)_3$, which diminishes its availability for ion exchange [43-44]. In contrast, for Schiff 2 (Fig. 7(b)) the optimal pH range was 5.0 as the adsorbed amounts of Cd(II) and Pb(II) ions were found to be 70 and 63 mg/g, respectively. At pH < 5, protonation of CSB and competition with H^+ ions reduce ion exchange efficiency, while at pH > 6, Zn(II) may hydrolyze, forming $Zn(OH)_2$, which limits its participation in the exchange process [45]. In both cases, the pH should be controlled to ensure the CSB remained deprotonated and available for binding while preventing the hydrolysis of the attached metal ions ((Fe(III) or Zn(II)) and the target metal ions (Cd(II) or Pb(II)) [46]. This balance ensures efficient ion exchange and high adsorption capacity for the target metals.

The point of zero charge (pH_{pzc}) plays a crucial role in determining the adsorption efficiency of modified CSB adsorbents for metal ions like Cd(II) and Pb(II). The pH_{pzc} of Schiff 1 was estimated to be 5.0, while Schiff 2 exhibited a lower pH_{pzc} of approximately 5.5. At a solution pH below the pH_{pzc}, the surface of the adsorbent remains positively charged due to protonation of active sites, leading to electrostatic repulsion with metal cations. However, as the solution pH increases beyond the pH_{pzc}, the surface gradually becomes negatively charged, enhancing electrostatic attraction between the adsorbent and metal ions. The optimal adsorption of Cd(II) and Pb(II) ions was observed at pH 4 for Schiff 1 and pH 5 for Schiff 2, suggesting that these pH conditions provided a favorable balance between sufficient deprotonation of functional groups and metal ion solubility. At these pH levels, the adsorbent surfaces likely carried a partial negative charge, facilitating strong electrostatic interactions and coordination with Cd(II) and Pb(II). Additionally, the presence of Zn and Fe modifications could influence local surface charge distribution and metal-binding affinity, further optimizing adsorption performance at these specific pH conditions.

Influence of time

Fig. 8(a) and 8(b) demonstrate the consequence of stirring duration on the adsorption of Cd(II) and Pb(II) ions using Schiffs 1 and 2 adsorbents. Experiments were conducted under static conditions over intervals ranging from 15 to 90 min. For Schiff 1, the adsorption of Cd(II) and Pb(II) ions increased and achieved equilibrium (83 and 77 mg/g, respectively) after 45 min. In contrast, Schiff 2 required 60 min to reach maximum adsorption for both ions. Beyond these timeframes, the adsorption of the target elements on both adsorbents slightly declined. Initially, the presence of available active sites and functional groups on Schiffs 1 and 2 facilitated rapid adsorption of the ions. However, as the active sites became occupied, the adsorption rate decreased significantly due to steric hindrance, which slowed the access of ions to

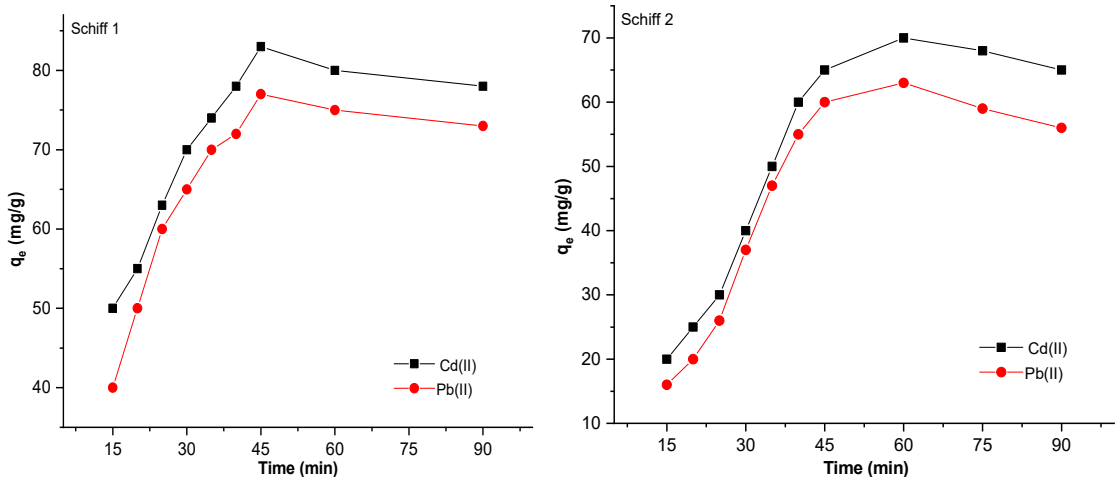

Fig 8. Effect of stirring time on the adsorption of Cd(II) and Pb(II) on Schiffs 1 and 2

remaining unoccupied sites. The adsorption processes for Cd(II) and Pb(II) on Schiffs 1 and 2 reached equilibrium at 45 and 60 min, respectively, establishing these durations as the optimal contact times for subsequent experiments.

Influence of concentration and temperature

Fig. 9 demonstrates the influence of initial concentration and temperature on the adsorption capacity of Cd and Pb ions using the prepared Schiff adsorbents while keeping other factors constant. Experiments were conducted with initial concentrations of Cd(II) and Pb(II) ranging from 25 to 100 mg/L and temperatures varying between 25 and 50 °C. The results revealed that raising the starting concentrations of Cd and Pb ions from 25 to 200 mg/L led to an enhancement in the adsorbed amounts to 96 mg/g for Cd(II) and 88 mg/g for Pb(II) on Schiff 1. For Schiff 2, the adsorbed amounts rose to 87 mg/g for Cd(II) and 79 mg/g for Pb(II). At lower metal ion concentrations, ample binding sites were accessible, whereas, at higher concentrations, the limited availability of binding sites caused more metal ions to remain in the solution, reducing adsorption efficiency. Besides, the adsorption of both the metals onto Schiff adsorbents was also enhanced with the decrease of temperature from 50 to 25 °C. The decrease of adsorption on the rise in temperature is suggestive of a chemisorption mechanism that hints towards the fact that the Cd(II)/Pb(II) interactions with adsorbents are exothermic in nature [47-48].

Adsorbent dose influence

Fig. 10(a) and 10(b) highlight the impact of adsorbent dosage by varying the weight of the two synthesized Schiff adsorbents between 10 and 50 mg.

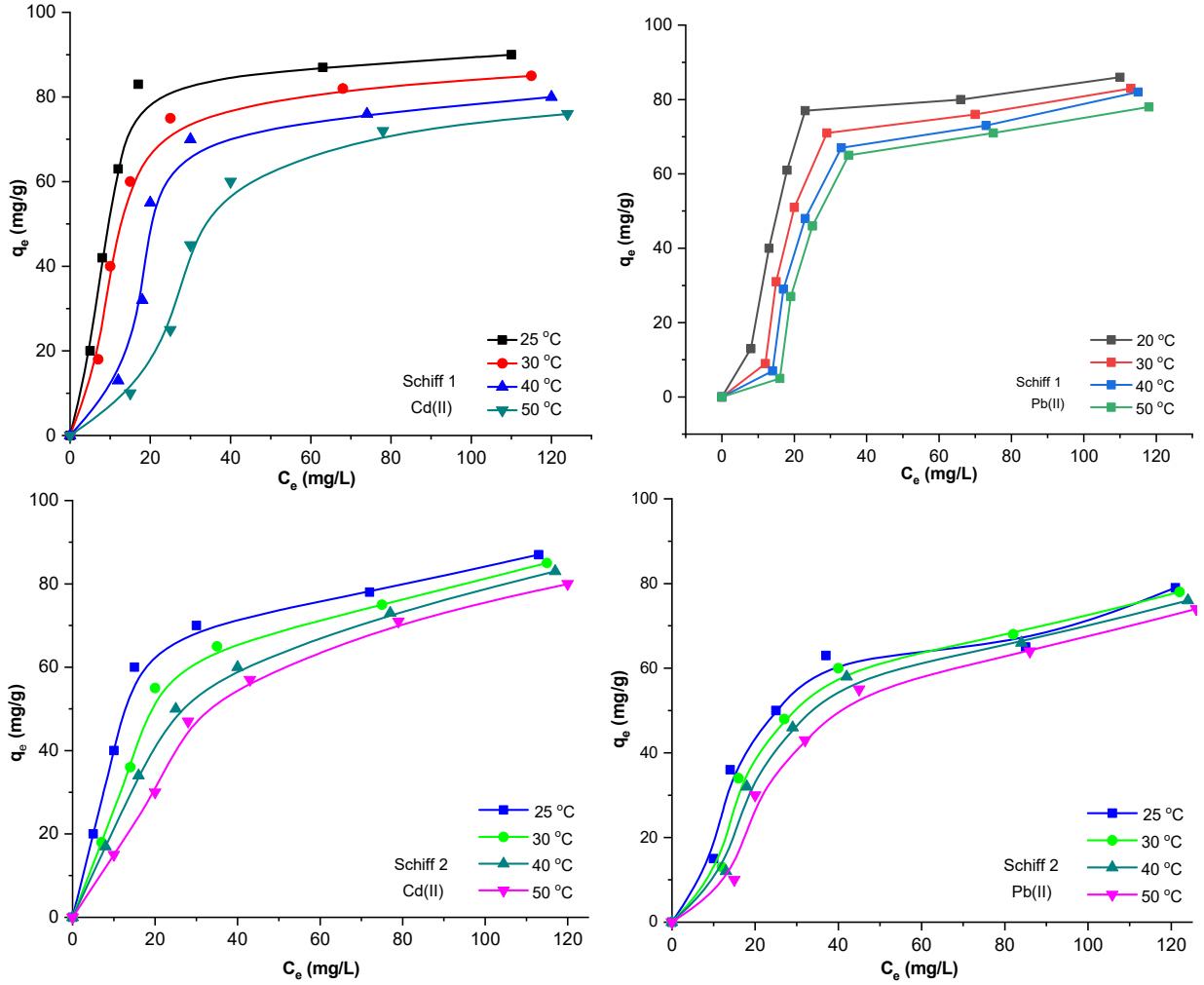

Fig 9. Effect of initial concentration and temperature on the Cd(II) and Pb(II) adsorption on Schiffs 1 and 2

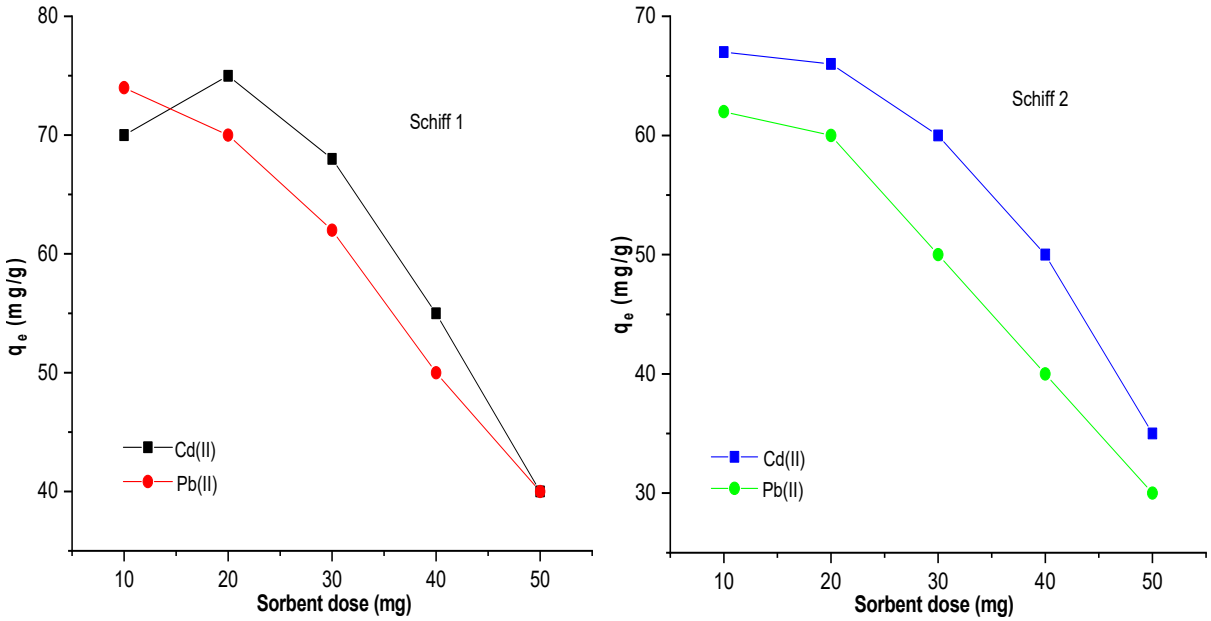

Fig 10. Effect of adsorbent amount on the adsorption of Cd(II) and Pb(II) on Schiffs 1 and 2

First, 25 mL solution containing 100 mg/L of Cd(II) and Pb(II) ions was used for the study, while all other conditions were kept consistent. Increasing the adsorbent weight from 10 to 50 mg resulted in a significant reduction in the uptake of Cd(II) and Pb(II) ions. With the concentration of the ions remaining unchanged, the observed reduction in uptake is likely due to the higher adsorbent weight, which provides more significant number of available adsorption sites. This site increase reduces the relative uptake of the ions.

Additionally, using smaller amounts of adsorbent can accumulate substances and spacer blockage, further hindering absorption. The buildup and steric hindrance enhance the diffusion of metal ions on the adsorbent surface. This effect is exacerbated by the limited surface area in low-dose adsorbents, resulting in insufficient overall surface area and reduced absorption efficiency.

Adsorption Kinetic Results

The predominant mechanism governing the adsorption of Cd(II) and Pb(II) ions onto the Schiff adsorbents was examined using two kinetic models: pseudo-first-order and pseudo-second-order. The rate-determining step for both models involved metal ions' adsorption onto the adsorbents' active sites. The kinetic modeling fitting curves and calculated parameters are presented in (Fig. 11) and detailed in Table 1.

The graphical representations in Fig. 11 and the derived parameters in Table 1 for both pseudo-first-order and pseudo-second-order kinetics indicate that the

Table 1. Quantitative measurements of the rate at which Cd and Pb ions are adsorbed onto Schiff adsorbents

Pseudo-1st-order	Schiff 1		Schiff 2	
	Cd(II)	Pb(II)	Cd(II)	Pb(II)
q_e (exp.)	83.0	77.0	70.0	63.0
q_e (cal.)	120.1	109.5	150.4	130.3
k_1	0.022	0.043	0.043	0.051
R^2	0.973	0.941	0.964	0.971
Pseudo-2nd-order				
q_e (cal.)	93.0	88.0	80.0	70.2
k_2	1.54×10^{-3}	3.11×10^{-3}	2.12×10^{-3}	3.53×10^{-3}
R^2	0.987	0.983	0.988	0.984

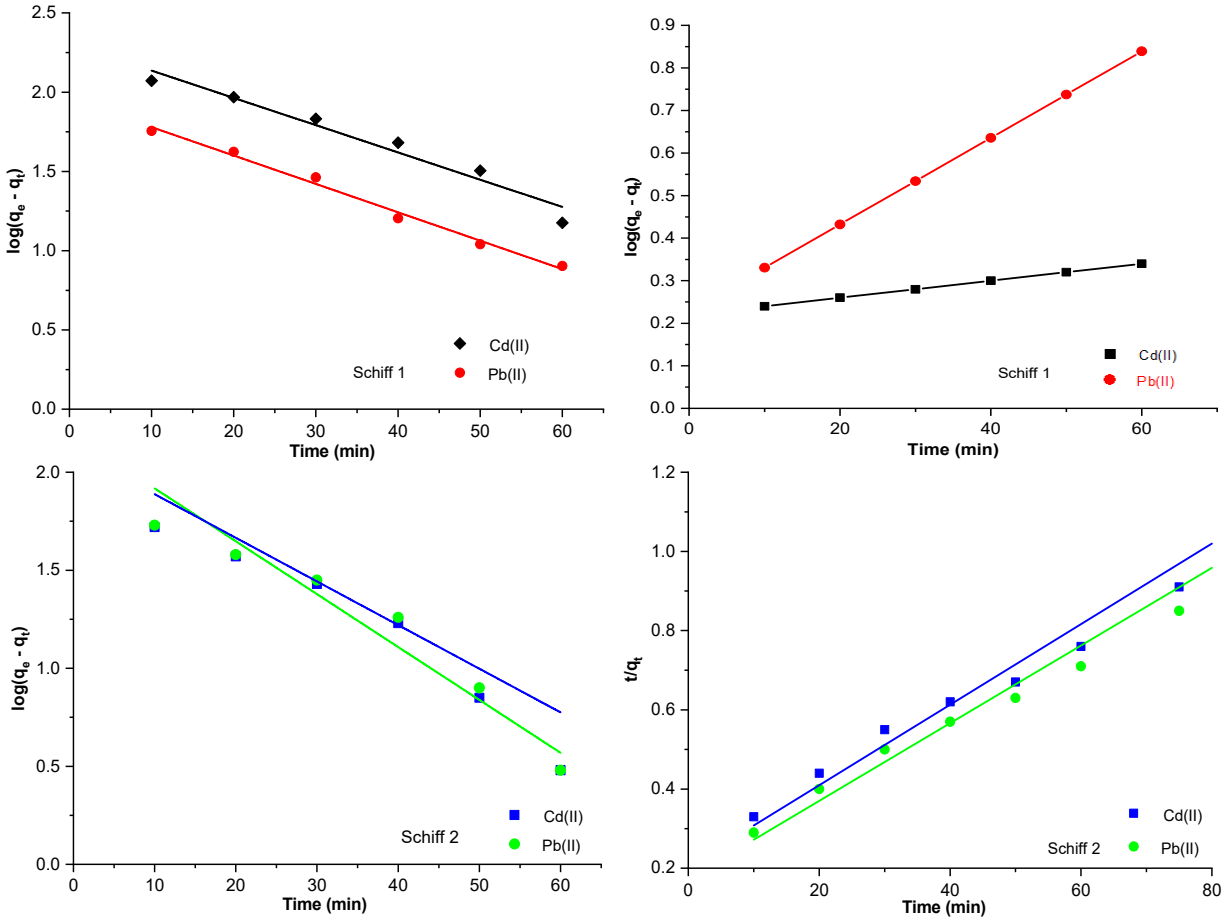

Fig 11. Kinetics modeling fitting Schiff 1 and 2 adsorbents

adsorption reaction mechanism is predominantly governed by the pseudo-second-order model. This conclusion is supported by the higher R^2 values for the pseudo-second-order model compared to the pseudo-first-order model for Cd(II) and Pb(II) ions on the synthesized adsorbents. Additionally, the calculated equilibrium adsorption capacities (q_e (cal.)) for pseudo-second-order kinetics closely align with the experimentally determined capacities (q_e (exp.)) for both Schiff adsorbents. This model implies that the adsorption rate is constrained by the valence forces responsible for electron sharing or exchange between the adsorbent and the adsorbate.

Adsorption mechanism

The CSB acts as a chelating agent, forming a complex with Fe(III) and Zn(II). When Cd(II) and Pb(II) were introduced, they displaced Fe and Zn from the complex due to competitive binding, forming a new complex with Cd and Pb separately and releasing Fe(II) and Zn(II) ions into the solution. The Cd(II) and Pb(II) selectivity of Fe(II) and Zn(II) in the CSB can be explained by applying the hard-soft acid-base theory (HSAB), supplemented with ionic radius-based rules. Cd(II) is a relatively softer acid in HSAB theory due to its relatively larger ionic radius, smaller charge density, and higher polarizability, whereas Fe(III) and Zn(II) are hard acids due to their smaller ionic radii, higher charge densities, and lower polarizability [49-50]. Nitrogen and oxygen are the donor atoms of the soft bases of CSB. Soft base donor atoms coordinate softer acids such as Cd(II) over harder acids such as Fe(III) and Zn(II). This is because there is increased orbital overlap and increased covalent interaction of the soft acid Cd(II) with the soft base CSB [42]. Furthermore, Cd(II) ionic radius (0.95 Å) is greater than Fe(III) (0.64 Å) and Zn(II) (0.74 Å) [50]. Due to its greater size, there is room for looser accommodation of

Table 2. Comparison of Schiff adsorbents uptakes with other adsorbents

Adsorbent material	Target metal	Uptake (mg/g)	Ref
Rice husk ash	Cd(II)	45.7	[54]
Biochar (sulfur-modified)		168	[55]
Zeolite (natural)		38.2	[56]
Graphene oxide/zeolite		195.7	[57]
Peat moss		88	[58]
This work		77 and 83	
Modified guar gum	Pb(II)	88	[59]
Functionalized silica nanoparticles		210	[60]
Orange peel		70	[61]
Groundnut shell		52	[62]
MOF-based composite		240	[63]
This work		63 and 70	

Cd(II) in the CSB coordination sphere, which is somewhat flexible due to its cellulose backbone.

Due to its intermediate Lewis acidity, Pb(II) readily competes with the harder Zn(II) and Fe(III) for complexation with the Schiff base ligand. The ability of these ligands to adjust their coordination geometry is particularly advantageous for accommodating the larger ionic radius of Pb(II) (1.19 Å), which is considerably greater than that of Fe(III) and Zn(II), ultimately leading to the formation of stable complexes [51-53].

Desorption and regeneration results

The primary objective of this study is to retrieve Cd and Pb ions adsorbed onto the Schiff adsorbents. Desorption experiments were conducted to better understand the adsorption mechanism, using HCl, HNO_3, H_2SO_4, and EDTA as eluting agents, as shown in (Fig. 12) Among these, nitric acid and EDTA demonstrated higher desorption efficiencies for Cd and Pb ions compared to H_2SO_4 and HCl. This is attributed to the strong chelating ability of EDTA and the relatively higher strength of HNO_3. For Cd, HNO_3 achieved 90 and 88% desorption efficiencies for Schiff 1 and 2, respectively, while for Pb, the efficiencies were 85 and 80%. However, complete recovery of both metal ions from the adsorbents was achieved using 1.0 M EDTA without damaging the adsorbents. This highlights 1.0 M EDTA as the most effective eluent for Cd and Pb ions, attributed to its multifunctional groups that form stable complexes with the metals, enabling efficient recovery. Furthermore,

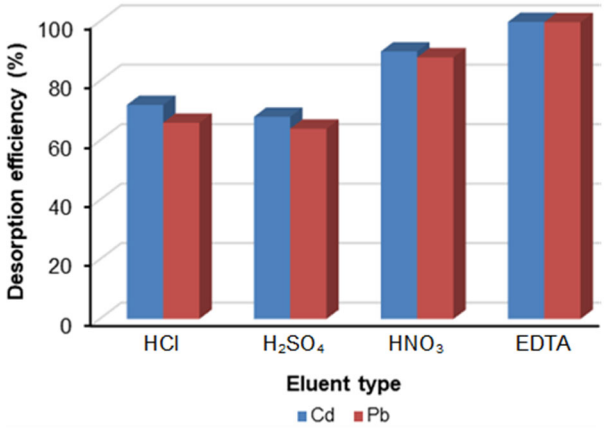

Fig 12. Desorption efficiency for Cd(II) and Pb(II)

four consecutive adsorption and desorption cycles for Cd and Pb ions were conducted on the Schiff adsorbents under the optimized conditions identified in this study. Table 2 emphasized comparison of the obtained uptakes of prepared Schiff adsorbents towards Cd and Pb ions compared to another adsorbent. It was concluded that these CSB adsorbents exhibited promising adsorption capacities for future wastewater treatment applications.

■ CONCLUSION

This study highlights the potential of CSB adsorbents, Schiffs 1 and 2, as efficient and sustainable materials for removing Cd and Pb ions from aqueous solutions. The synthesis and characterization of these adsorbents demonstrated improved surface properties and the presence of active sites, contributing to their high efficiency in heavy metal adsorption. The

adsorption mechanism exhibited characteristics of chemisorption, following pseudo-second-order kinetics. The maximum monolayer adsorption capacities were determined to be 83 mg/g for Cd and 77 mg/g for Pb on Schiff 1, while Schiff 2 demonstrated capacities of 70 mg/g for Cd and 63 mg/g for Pb. Optimal adsorption conditions included a feed solution pH of 4.0 for Cd and 5.0 for Pb, stirring durations of 45 and 60 min for Cd and Pb ions, a metal ion concentration of 100 mg/L, and room temperature (25 ± 2 °C). Additionally, EDTA was identified as an effective desorbing agent, facilitating the recovery of Cd and Pb ions over 4 consecutive cycles. These results emphasize the potential of modified CSB adsorbents as cost-effective and environmentally friendly solutions for addressing heavy metal contamination in wastewater treatment applications.

■ ACKNOWLEDGMENTS

The Chemistry Department of Al-Nahrain University's College of Science is acknowledged by the author for its assistance in this study.

■ CONFLICT OF INTEREST

The author has no conflict of interest.

■ REFERENCES

[1] Li, C., Yu, Y., Fang, A., Feng, D., Du, M., Tang, A., Chen, S., and Li, A., 2022, Insight into biosorption of heavy metals by extracellular polymer substances and the improvement of the efficacy: A review, *Lett. Appl. Microbiol.*, 75 (5), 1064–1073.

[2] Rajendran, S., Priya, A.K., Senthil Kumar, P., Hoang, T.K.A., Sekar, K., Chong, K.Y., Khoo, K.S., Ng, H.S., and Show, P.L., 2022, A critical and recent developments on adsorption technique for removal of heavy metals from wastewater-A review, *Chemosphere*, 303 (Pt. 2), 135146.

[3] Okatch, H., Ghimirey, A., Lam, H., Nkala, J.J., Raseipei, P., and Regis, N., 2023, Identifying contextually relevant lead exposures and risk practices/behaviors in Botswana and assessing caregiver lead knowledge levels, *Cogent Public Health*, 10 (1), 2211725.

[4] Nam, Y.S., Alex-Oni, K., Fitzstevens, M., Patel, K., and Hore, P., 2025, Advancing public health interventions: A novel surveillance system for hazardous consumer products, *J. Public Health Manage. Pract.*, 31 (3), 372–376.

[5] Ibrahim, F.M., Najeeb, D.A., and ThamerSadeq, H., 2023, Green preparation of Cu nanoparticles of the avocado seed extract as an adsorbent surface, *Mater. Sci. Energy Technol.*, 6, 130–136.

[6] Razzak, S.A., Faruque, M.O., Alsheikh, Z., Alsheikhmohamad, L., Alkuroud, D., Alfayez, A., Hossain, S.M.Z., and Hossain, M.M., 2022, A comprehensive review on conventional and biological-driven heavy metals removal from industrial wastewater, *Environ. Adv.*, 7, 100168.

[7] Kumar, P., Abbas, Z., Kumar, P., Das, D., and Mobin, S.M., 2024, Highlights in interface of wastewater treatment by utilizing metal organic frameworks: Purification and adsorption kinetics, *Langmuir*, 40 (10), 5040–5059.

[8] Yuan, Y., Li, R., and Peng, S., 2023, Research progress on chemical modification of waste biomass cellulose to prepare heavy metal adsorbents, *Polym. Bull.*, 80 (11), 11671–11700.

[9] Rashid, R., Shafiq, I., Akhter, P., Iqbal, M.J., and Hussain, M., 2021, A state-of-the-art review on wastewater treatment techniques: The effectiveness of adsorption method, *Environ. Sci. Pollut. Res.*, 28 (8), 9050–9066.

[10] Alhaithloul, H.A.S., Alsudays, I.M., Zaki, E.G., Elsaeed, S.M., Mubark, A.E., Salib, L., Safwat, G., Niedbała, G., Diab, A., Abdein, M.A., Alharthi, A., Zakai, S.A., and Elkelish, A., 2024, Retrieval of Cu^{2+} and Cd^{2+} ions from aqueous solutions using sustainable guar gum/PVA/montmorillonite nanocomposite films: Effect of temperature and adsorption isotherms, *Front. Chem.*, 12, 1393791.

[11] Annu, A., Mittal, M., Tripathi, S., and Shin, D.K., 2024, Biopolymeric nanocomposites for wastewater remediation: An overview on recent progress and challenges, *Polymers*, 16 (2), 294.

[12] Ibrahim, F.M., and Abdalhadi, S.M., 2021,

Performance of Schiff bases metal complexes and their ligand in biological activity: A review, *Al-Nahrain J. Sci.*, 24 (1), 1–10.

[13] Etale, A., Onyianta, A.J., Turner, S.R., and Eichhorn, S.J., 2023, Cellulose: A review of water interactions, applications in composites, and water treatment, *Chem. Rev.*, 123 (5), 2016–2048.

[14] Ahmad, S.M., Ibrahim, F.M., Adnan Hasan, A., Mawlood Mikhlif, H., Saad Jwad, R., Alhuwaymil, Z., Alshareef, S.A., Alyami, M.S.S., Al-Mashhadani, M.H., and Kommanaboyina, S., 2024, Fluorescent properties of chitosan-stabilized bisdemethoxycurcumin-silver nanoparticles: Synthesis and characterization, *Results Chem.*, 10, 101719.

[15] Kaur, J., Sengupta, P., and Mukhopadhyay, S., 2022, Critical review of bioadsorption on modified cellulose and removal of divalent heavy metals (Cd, Pb, and Cu), *Ind. Eng. Chem. Res.*, 61 (5), 1921–1954.

[16] Olawale, S.A., Bonilla-Petriciolet, A., Mendoza-Castillo, D.I., Okafor, C.C., Sellaoui, L., and Badawi, M., 2022, Thermodynamics and mechanism of the adsorption of heavy metal ions on keratin biomasses for wastewater detoxification, *Adsorpt. Sci. Technol.*, 2022, 7384924.

[17] Abd El-Sayed, E.S., Dacrory, S., Essawy, H.A., Ibrahim, H.S., Ammar, N.S., and Kamel, S., 2023, Sustainable grafted chitosan-dialdehyde cellulose with high adsorption capacity of heavy metal, *BMC Chem.*, 17 (1), 117.

[18] Yue, X., Huang, J., Jiang, F., Lin, H., and Chen, Y., 2019, Synthesis and characterization of cellulose-based adsorbent for removal of anionic and cationic dyes, *J. Eng. Fibers Fabr.*, 14, 1558925019828194.

[19] Sharma, P., Jain, R., Premi, A., Kumar, N., and Parashar, A., 2022, Linear and non-linear regression analysis for the sorption kinetics of Tropaeoline 000 onto nano talc, *Int. J. Environ. Anal. Chem.*, 102 (9), 2152–2167.

[20] Ben Haj Fraj, S., Ferlazzo, S., El Haskouri, A., Neri, J., and Baouab, M.H.V., 2023, New fluorescent Schiff base modified nanocellulose-based chemosensors for the selective detection of Fe^{3+}, Zn^{2+} and Cu^{2+} in semi-aqueous media and application in seawater sample, *Int. J. Biol. Macromol.*, 253, 127762.

[21] Ren, L., Yang, Z., Huang, L., He, Y., Wang, H., and Zhang, L., 2020, Macroscopic poly Schiff base-coated bacteria cellulose with high adsorption performance, *Polymers*, 12 (3), 714.

[22] Sun, Q., Dong, X., Meng, Q., Xu, J., and Wang, T., 2024, Reversible Schiff base chemistry in arginine-grafted regenerated cellulose hydrogel: Integration of chitosan and zinc ions for enhanced hemostasis, antibacterial action, and accelerated wound healing, *ACS Appl. Bio Mater.*, 7 (10), 7030–7039.

[23] Alhalili, Z., and Abdelrahman, E.A., 2024, Efficient removal of Zn(II) ions from aqueous media using a facilely synthesized nanocomposite based on chitosan Schiff base, *Sci. Rep.*, 14 (1), 17598.

[24] Kumar, R., and Sharma, R.K., 2019, Synthesis and characterization of cellulose based adsorbents for removal of Ni(II), Cu(II) and Pb(II) ions from aqueous solutions, *React. Funct. Polym.*, 140, 82–92.

[25] Xu, Y., Shi, Y., Lei, F., and Dai, L., 2020, A novel and green cellulose-based Schiff base-Cu(II) complex and its excellent antibacterial activity, *Carbohydr. Polym.*, 230, 115671.

[26] Meng, P., Zhang, T., Su, Y., Peng, D., Zhou, Q., Zeng, H., Yu, H., Lun, L., Zhang, N., Zhang, L., and Zheng, L., 2024, Cellulose-based materials in the treatment of wastewater containing heavy metal pollution: Recent advances in quantitative adsorption mechanisms, *Ind. Crops Prod.*, 217, 118825.

[27] Elwakeel, K.Z., Elgarahy, A.M., and Mohammad, S.H., 2017, Magnetic Schiff's base sorbent based on shrimp peels wastes for consummate sorption of chromate, *Water Sci. Technol.*, 76 (1), 35–48.

[28] Kaur, M., Kumar, S., Yusuf, M., Lee, J., Malik, A.K., Ahmadi, Y., and Kim, K.H., 2023, Schiff base-functionalized metal-organic frameworks as an efficient adsorbent for the decontamination of heavy metal ions in water, *Environ. Res.*, 236, 116811.

[29] Son, D., Cho, S., Nam, J., Lee, H., and Kim, M., 2020, X-ray-based spectroscopic techniques for

characterization of polymer nanocomposite materials at a molecular level, *Polymers*, 12 (5), 1053.

[30] Saberi-Zare, M., and Bodaghifard, M.A., 2025, A Schiff base-functionalized chitosan magnetic bio-nanocomposite for efficient removal of Pb(II) and Cd(II) ions from aqueous solutions, *Int. J. Biol. Macromol.*, 296, 139794.

[31] Kenawy, E.R., Azaam, M.M., Afzal, M., Khatoon, A., Ansari, M.T., and Hasnain, M.S., 2020, "Pharmaceutical Application of Cellulose Derivatives" in *Tailor-Made Polysaccharides in Biomedical Applications*, Eds. Nayak, A., Hasnain, M.S., and Aminabhavi, T., Academic Press, Cambridge, MA, US, 305–328.

[32] Poletto, M., Pistor, V., and Zattera, A.J., 2013, "Structural Characteristics and Thermal Properties of Native Cellulose" in *Cellulose - Fundamental Aspects*, Eds. Van De Ven, T.G.M., and Godbout, L., IntechOpen, Rijeka, Croatia.

[33] Verma, C., Singh, V., and AlFantazi, A., 2024, Cellulose, cellulose derivatives and cellulose composites in sustainable corrosion protection: Challenges and opportunities, *Phys. Chem. Chem. Phys.*, 26 (15), 11217–11242.

[34] Jenisha, J., David, S.T., and Priyadharsini, J.P., 2015, Schiff base ligand its complexes and their FT-IR spectroscopy studies, *Int. J. Appl. Bioeng.*, 9 (1), 1–4.

[35] Fakhre, N.A., and Ibrahim, B.M., 2018, The use of new chemically modified cellulose for heavy metal ion adsorption, *J. Hazard. Mater.*, 343, 324–331.

[36] Saravanan, R., and Ravikumar, L., 2015, The use of new chemically modified cellulose for heavy metal ion adsorption and antimicrobial activities, *J. Water Resour. Prot.*, 7 (6), 530–545.

[37] Coates, J., 2006, "Interpretation of Infrared Spectra, A Practical Approach" in *Encyclopedia of Analytical Chemistry*, John Wiley & Sons, Hoboken, New Jersey, US.

[38] Patil, M.K., Masand, V.H., and Maldhure, A.K., 2021, Schiff base metal complexes precursor for metal oxide nanomaterials: A review, *Curr. Nanosci.*, 17 (4), 634–645.

[39] Oyewo, O.A., Nevondo, N.G., Onwudiwe, D.C., and Onyango, M.S., 2021, Photocatalytic degradation of methyl blue in water using sawdust-derived cellulose nanocrystals-metal oxide nanocomposite, *J. Inorg. Organomet. Polym. Mater.*, 31 (6), 2542–2552.

[40] Di Bernardo, P., Zanonato, P.L., Tamburini, S., Tomasin, P., and Vigato, P.A., 2006, Complexation behaviour and stability of Schiff bases in aqueous solution. The case of an acyclic diimino(amino) diphenol and its reduced triamine derivative, *Dalton Trans.*, (39), 4711–4721.

[41] Gharamaleki, J.A., Akbari, F., Karbalaei, A., Ghiassi, K.B., and Olmstead, M.M., 2016, Synthesis, characterization and crystal structure of a new Schiff base ligand from a bis(thiazoline) template and hydrolytic cleavage of the imine bond induced by a Co(II) cation, *Open J. Inorg. Chem.*, 6 (1), 76–88.

[42] Wang, L.K., Wang, M.H.S., Hung, Y.T., Shammas, N.K., and Chen, J.P., 2017, *Handbook of Advanced Industrial and Hazardous Wastes Management*, 1st Ed., CRC Press, Boca Raton, FL, US.

[43] Kyzas, G.Z., and Matis, K.A., 2015, Nanoadsorbents for pollutants removal: A review, *J. Mol. Liq.*, 203, 159–168.

[44] Bhatnagar, A., and Sillanpää, M., 2010, Utilization of agro-industrial and municipal waste materials as potential adsorbents for water treatment—A review, *Chem. Eng. J.*, 157 (2-3), 277–296.

[45] Khalil, M.M.H., Ismail, E.H., Mohamed, G.G., Zayed, E.M., and Badr, A., 2012, Synthesis and characterization of a novel Schiff base metal complexes and their application in determination of iron in different types of natural water, *Open J. Inorg. Chem.*, 2 (2), 13–21.

[46] Barakat, M.A., 2011, New trends in removing heavy metals from industrial wastewater, *Arabian J. Chem.*, 4 (4), 361–377.

[47] Somorjai, G.A., and Li, Y., 2010, *Introduction to Surface Chemistry and Catalysis*, John Wiley & Sons, Hoboken, NJ, US.

[48] Foo, K.Y., Hameed, B.H., 2010, Insights into the modelling of adsorption isotherm systems, *Chem. Eng. J.*, 156 (1), 2–10.

[49] Mardani, H.R., Ravari, F., Kalaki, A., and Hokmabadi, L., 2020, New Schiff-base's modified chitosan: Synthesis, characterization, computational, thermal study and comparison on adsorption of copper(II) and nickel(II) metal ions in aqueous, *J. Polym. Environ.*, 28 (9), 2523–2538.

[50] Nyamato, G.S., Kabogo, I.T., Maqinana, S., Bachmann, R., Schmitz, M., Ogunah, J., Kleist, W., and Ojwach, S.O., 2024, Removal, mechanistic and kinetic studies of Cr(VI), Cd(II), and Pb(II) cations using Fe_3O_4 functionalized Schiff base chelating ligands, *Environ. Sci. Pollut. Res.*, 31 (54), 63374–63392.

[51] El Mahdaoui, A., Radi, S., Elidrissi, A., Faustino, M.A.F., Neves, M.G.P.M.S., and Moura, N.M.M., 2024, Progress in the modification of cellulose-based adsorbents for the removal of toxic heavy metal ions, *J. Environ. Chem. Eng.*, 12 (5), 113870.

[52] Ho, Y.S., and McKay, G., 1999, Pseudo-second order model for sorption processes, *Process Biochem.*, 34 (5), 451–465.

[53] Zayed, E.M., Zayed, M.A., and Hindy, A.M.M., 2014, Thermal and spectroscopic investigation of novel Schiff base, its metal complexes, and their biological activities, *J. Therm. Anal. Calorim.*, 116 (1), 391–400.

[54] Naiya, T.K., Bhattacharya, A.K., Mandal, S., and Das, S.K., 2009, The sorption of lead(II) ions on rice husk ash, *J. Hazard. Mater.*, 163 (2-3), 1254–1264.

[55] Chen, D., Wang, X., Wang, X., Feng, K., Su, J., and Dong, J., 2020, The mechanism of cadmium sorption by sulphur-modified wheat straw biochar and its application cadmium-contaminated soil, *Sci. Total Environ.*, 714, 136550.

[56] Kazemian, H., Gedik, K., and İmamoğlu, İ., 2012, "Environmental Applications of Natural Zeolites" in *Handbook of Natural Zeolites*, Bentham Science Publishers, Sharjah, UAE, 473–508.

[57] Carmalin Sophia, A., Arfin, T., and Lima, E.C., 2019, "Recent Developments in Adsorption of Dyes Using Graphene Based Nanomaterials" in *A New Generation Material Graphene: Applications in Water Technology*, Eds. Naushad, M., Springer, Cham, Switzerland, 439–471.

[58] Sutherland, C., and Venkobachar, C., 2020, Regeneration of a chemically improved peat moss for the removal and recovery of Cu(II) and Pb(II) from aqueous solution, *Desalin. Water Treat.*, 178, 172–181.

[59] Mubark, A.E., Zaki, E.G., Hakem, H.A., Abdel-Rahman, A.A.H., Elsaeed, S.M., and Elkelish, A., 2025, Guar gum hydrogel as a biosorbent for Cd(II) and Cu(II) ions: Kinetic, equilibrium, and thermodynamic insights, *ChemistrySelect*, 10 (3), e202404817.

[60] Hasankola, Z.S., Rahimi, R., and Safarifard, V., 2019, Rapid and efficient ultrasonic-assisted removal of lead(II) in water using two copper-and zinc-based metal-organic frameworks, *Inorg. Chem. Commun.*, 107, 107474.

[61] Molaudzi, N.R., and Ambushe, A.A., 2022, Sugarcane bagasse and orange peels as low-cost biosorbents for the removal of lead ions from contaminated water samples, *Water*, 14 (21), 3395.

[62] Kumar, S., Gunasekar, V., and Ponnusami, V., 2013, Removal of methylene blue from aqueous effluent using fixed bed of groundnut shell powder, *J. Chem.*, 2013 (1), 259819.

[63] Darabdhara, J., and Ahmaruzzaman, M., 2022, Recent developments in MOF and MOF based composite as potential adsorbents for removal of aqueous environmental contaminants, *Chemosphere*, 304, 135261.